Neurochemical Research (2023) 48:3084–3098
https://doi.org/10.1007/s11064-023-03968-y

ORIGINAL PAPER

VCAM-1$^+$ hUC-MSCs Exert Considerable Neuroprotection Against Cerebral Infarction in Rats by Suppression of NLRP3-Induced Pyroptosis

Xiao Zhang[1] · Xiaoyu Sang[1] · Yanting Chen[1] · Hao Yu[2] · Yuan Sun[3] · Xilong Liang[4] · Xiaolei Zheng[1] · Xiao Wang[1] · Hui Yang[1] · Jianzhong Bi[1] · Leisheng Zhang[5,6,7] · Ping Wang[1]

Received: 27 March 2023 / Revised: 7 June 2023 / Accepted: 8 June 2023 / Published online: 19 June 2023

Abstract

Mesenchymal stem/stromal cells (MSCs) are spindle-like heterogeneous cell populations with advantageous bidirectional immunomodulatory and hematopoietic support effects. Vascular cellular adhesion molecule-1 (VCAM-1)$^+$ MSCs have been reported to exhibit immunoregulatory and proangiogenic capacities. Here, we studied the effects of VCAM-1$^+$ human umbilical cord (hUC)-MSCs on neuroprotection against cerebral infarction. Sprague–Dawley rats were subjected to middle cerebral artery occlusion (MCAO), and VCAM-1$^-$ and VCAM-1$^+$ hUC-MSCs were intravenously injected into the rat 4 h post-MCAO surgery. Thereafter, modified neurological severity scores (mNSS) were determined, and the Morris water maze test, 2,3,5-triphenyltetrazolium chloride (TTC), hematoxylin and eosin (H&E), Nissl, TUNEL staining, and qRT-PCR were conducted. Following induction of oxygen–glucose deprivation/reoxygenation (OGD/R), SH-SY5Y cells were co-cultured with VCAM-1$^-$ and VCAM-1$^+$ hUC-MSCs. CCK-8, flow cytometry, ELISA, and western blot analyses were performed in vitro. Compared with VCAM-1$^-$ hUC-MSCs, administration of VCAM-1$^+$ hUC-MSCs revealed improved therapeutic efficacy against cerebral infarction in rats, as confirmed by lower mNSS scores and infarct volumes, as well as improved learning and memory capacities. In addition, VCAM-1$^+$ hUC-MSCs exhibited improved efficacy against neurological defects in rats with cerebral infarction, accompanied by inhibition of the NLRP3-mediated inflammatory response. VCAM-1$^+$ hUC-MSC co-culture improved the viability and diminished NLRP3-mediated inflammatory response in OGD/R-treated SH-SY5Y cells. Moreover, NLRP3 overexpression in SH-SY5Y cells prevented the beneficial effects of VCAM-1$^+$ hUC-MSC co-culture. Overall, our findings demonstrated the relevance of VCAM-1$^+$ hUC-MSC-based cytotherapy for preclinical neuroprotection against cerebral infarction.

Keywords VCAM-1 · hUC-MSCs · Cerebral infarction · Neuroprotective effect · NLRP3

Abbreviations

MSCs	Mesenchymal stem/stromal cells
hUC-MSCs	Human umbilical cord MSCs
PSC	Pluripotent stem cells
NLRP3	NOD-like receptor thermal protein domain-associated protein 3
ASC	Apoptosis associated speck like protein containing CARD
VCAM-1	Vascular cellular adhesion molecule-1
EAM	Experimental autoimmune myocarditis
DEGs	Differentially expressed genes
GO	Gene ontology
mNSS	Modified neurological severity scores
MCAO	Middle cerebral artery occlusion
OGD/R	Oxygen-glucose deprivation/reoxygenation
FCM	Flow cytometry
NDA	New drug application
GSEA	Gene set enrichment analysis
PFA	Paraformaldehyde
WHO	World Health Organization
MCA	Middle cerebral artery
qRT-PCR	Quantitative real-time polymerase chain reaction
ELISA	Enzyme-linked immunosorbent assay
sEVs	Small extracellular vesicles

Extended author information available on the last page of the article

Introduction

Cerebral infarction is the leading cause of disability and death worldwide [1]. The World Health Organization (WHO) estimated that stroke due to cerebral infarction caused 5.7 million deaths worldwide in 2005, accounting for 9.9% of all deaths [2]. Cerebral infarction is a multifactorial disease associated with diverse risk factors, including age, smoking, diabetes mellitus, hypertension, obesity, and obstructive sleep apnea [3, 4]. Timely reperfusion with intravenous thrombolysis and/or endovascular thrombectomy is an effective treatment for stroke in the clinic [5]; however, only a small proportion of patients (10%–20%) with stroke reach the hospital within 3 h [6]. Therefore, neurorestoration after cerebral infarction has been recognized as the primary management goal [7].

Mesenchymal stem/stromal cells (MSCs) are spindle-like heterogeneous cell populations with advantageous bidirectional immunomodulation and hematopoietic-supporting effects, together with a unique multi-lineage differentiation capacity towards adipocytes, osteoblasts, and chondrocytes [8–10]. As a key component of the microenvironment, MSCs and their derivatives (e.g., exosomes and small extracellular vesicles) are thought to play a pivotal role in the intervention of various relapsed and recurrent diseases such as acquired aplastic anemia [11, 12], acute myelogenous leukemia (AML) [13], Crohn's disease [14], osteoarthritis [15], primary ovarian insufficiency [16], and neurological diseases [17]. To date, MSCs with heterogeneity have been derived from perinatal tissues (e.g., the umbilical cord, placental chorionic villi, and amniotic membrane) [9, 18], adult tissues (e.g., adipose tissue and bone marrow) [13, 19], and even pluripotent stem cells (PSCs) (e.g., induced PSCs and embryonic stem cells) [20, 21]. Umbilical cord MSCs (UC-MSCs) are a rich source of MSCs, and they are more primitive, proliferative, and immunosuppressive than their adult counterparts [22]. They also have additional advantages, such as no need for bone marrow aspiration and higher self-renewal capacities [23]. Accumulating evidences showed that UC-MSCs may have potentials for use in the clinic treatment of several human diseases, including cerebral infarction [24, 25]. Notably, we and other pioneering investigators in this field have identified subsets of MSCs with remarkable characteristics for more efficient disease management. For instance, Wei et al. and Du et al. have reported highly efficient generation of VCAM-1^+ perinatal MSCs with improved immunoregulatory [12] and proangiogenic capacities [26], respectively. Despite the potential superiority of VCAM-1^+ hUC-MSCs in increasing neuronal survival and decreasing levels of inflammatory cytokines in stroke models, yet the impact of the aforementioned VCAM-1^+ MSCs in neuroprotection against cerebral infarction is largely unknown.

The NOD-like receptor thermal protein domain-associated protein 3 (NLRP3) inflammasome is a cytosolic protein complex composed of NLRP3, apoptosis-associated speck like protein containing CARD (ASC), and caspase-1 [27]. Cleaved caspase-1 promotes maturation of interleukin (IL)-1β and IL-18 and triggers pyroptosis [27]. The NLRP3 inflammasome contributes to the pathogenesis of several human diseases, including diabetes [28], osteoporosis [29], liver disease [30], and cardiovascular diseases [31]. Inhibition of the NLRP3 inflammasome has the potential to relieve neuroinflammation and brain injury in experimental stroke models [32, 33].

In this work, we used a rat model of cerebral infarction to evaluate the therapeutic effects of VCAM-1^+ hUC-MSCs administered by intravenous injection. Strikingly, the pathological manifestations of rats with administration of VCAM-1^+ hUC-MSCs revealed improved neuroprotection over those with the VCAM-1^- hUC-MSCs counterpart. NLRP3-induced pyroptosis and pathological deterioration during cerebral infarction were rescued by VCAM-1^+ hUC-MSC-based cytotherapy.

Material and Methods

Generation of VCAM-1^- UC-MSCs and VCAM-1^+ UC-MSCs

VCAM-1^- UC-MSCs and VCAM-1^+ UC-MSCs at passage 3 were purchased from Health-Biotech (Tianjin) Stem Cell Institute Co., Ltd. and identified by flow cytometry (FCM) assay as we previously described [9]. VCAM-1^- UC-MSCs were cultured in DMEM-F12 basal medium (HyClone, Logan, UT, USA) supplemented with 10% FBS (Gibco, Grand Island, NY, USA), 1% penicillin–streptomycin (Gibco), 1% L-glutamine (Gibco), 1 × NEAA (Gibco), 2 ng/mL bFGF (PeproTech), and 10 ng/mL EGF (PeproTech). For VCAM-1^+ UC-MSCs generation, VCAM-1^- UC-MSCs (5×10^5 cells/mL) were cultured in MSC culture medium for 24 h, followed by the addition of 10 ng/mL recombinant human IL-1β (rhIL-1β, PeproTech), 10 ng/mL recombinant human IL-4 (rhIL-4, PeproTech), and 20 ng/mL recombinant human IFN-γ (rhIFN-γ, PeproTech) for 48 h at 37℃, in 5% CO_2 as we previously reported [12]. The indicated cytokines are listed in Additional file 1: Additional Information: Additional Table S1.

RNA-SEQ and Bioinformatics Analyses

VCAM-1^- UC-MSCs and VCAM-1^+ UC-MSCs (3 independent UC-MSCs) were lysed with TRIZol® reagent

(Invitrogen), and total mRNAs were extracted according to the manufacturer's instructions, as we recently reported [13]. After assessment of the purity by NanoDrop™ (ThermoFisher Scientific), the total mRNAs were sequenced by Novogene (Tianjin, China). Bioinformatics analyses were then conducted using databases and online platforms [11, 13]. Signaling pathway analyses were carried out based on the Kyoto Encyclopedia of Genes and Genomes (KEGG) website (https://www.kegg.jp/), the Gene Ontology (GO) assay was conducted using the GO website (http://geneontology.org/), and gene set enrichment analysis (GSEA) was carried out using the GSEA website (https://www.gsea-msigdb.org/gsea/index.jsp).

Rat Model of Middle Cerebral Artery Occlusion (MCAO)

Male Sprague–Dawley rats (8 weeks old, weighing 280–300 g, N = 5 per group) were purchased from Ji'nan Pengyue Experimental Animal Breeding Co., Ltd. (Jinan, China) for random grouping. After one week of habituation to standard cages, MCAO surgery was performed. The rats had free access to food and water with a 12 h light/dark cycle and environmental conditions of 22 ± 2 °C and 60 ± 5% humidity. Before surgery, the rats were fasted for 10 h but had access to water. After anesthetization with 2% pentobarbital sodium (i.p., 0.3 mL/100 g), all 5 rats in each group were placed on a thermal insulation blanket and a 2–3 cm incision was made in the middle of the neck. The right common carotid artery (CCA), internal carotid artery (ICA), and external carotid artery (ECA) were exposed, and the middle cerebral artery (MCA) was occluded using a 4–0 nylon suture with a round tip. Two hours later, the suture was removed to induce reperfusion injury. The rats in the sham group underwent the same procedure without occlusion of the middle cerebral artery. Rats were intraperitoneally injected with penicillin (40,000 U per rat) to avoid infection. The animal studies were approved by the Ethics Committee of the Institutional Animal Care and Use Committee of the Second Hospital of Shandong University in accordance with the National Institutes of Health (NIH) guidelines for the Care and Use of Laboratory Animals.

Animal Grouping and UC-MSCs Transplantation

The rats were randomly divided into four groups (five rats per group): Sham, MCAO, MCAO + VCAM-1$^-$, and MCAO + VCAM-1$^+$. The rats in the Sham and MCAO groups underwent surgery as described above and received a tail vein injection of 1 × PBS 4 h post-surgery. The rats in MCAO + VCAM-1$^-$ and MCAO + VCAM-1$^+$ groups underwent MCAO surgery and received a tail vein injection of VCAM-1$^-$ or VCAM-1$^+$ UC-MSCs (4×10^6 cells/rat) 4 h post-surgery.

Neurological Evaluation

Neurological deficits were evaluated using the modified neurological severity score (mNSS) at 1 and 14 days after MCAO surgery. The mNSS was graded on a scale of 1–18 with the following five tests: flexion of limbs and head movement after raising the rat by the tail (3 points), ability to stand and/or walk after placing the rat on the floor (3 points), sensory tests (2 points), beam balance tests (6 points), and reflexes absent and abnormal movements (4 points).

Morris Water Maze Test

The Morris water maze test was performed at 1, 2, 3, 4, and 5 days post-surgery, as previously described [34, 35], in a circular pool filled with water at 25 ± 1 °C. The circular pool was divided into four quadrants through the midline, and the platform was set 1 cm below the water surface. The rats were gently placed into the pool and allowed to find the platform within 60 s. Rats were kept on the platform for 30 s before being released. Escape latency, the time spent in the target quadrant, and the crossing time were recorded.

2,3,5-Triphenyltetrazolium Chloride (TTC) Staining

At 14 days post-MCAO, the rats were anesthetized by intraperitoneal injection of 2% pentobarbital sodium and sacrificed by exsanguination from the aorta abdominalis. The brain tissues were collected and placed at – 20 °C for 30 min. After being cut into 2 mm-thick slices, the sections were incubated with 2% TTC solution (Sigma-Aldrich, St. Louis, MO, USA) for 30 min at 37 °C in the dark. The tissues were fixed with 4% paraformaldehyde (PFA) for 24 h, and the infarct volumes were analysed using ImageJ software (National Institutes of Health) according to a method previously reported [36].

Hematoxylin and Eosin (H&E) Staining

Brain tissues were fixed with 4% PFA for 24 h, embedded in paraffin, and cut into 5 µm-thick sections. The tissue sections were stained using an H&E Staining Kit (Beyotime, Shanghai, China). Briefly, the tissue sections were stained with hematoxylin for 10 min, washed with water for 10 min, and then stained with eosin for 30 s at room temperature (RT). The sections were placed in increasing concentrations of ethyl alcohol (70, 80, 90, and then 100%) for 10 s each, followed by xylene for 5 min at RT. Images were captured using a light microscope (Nikon Corporation) in all 5 rats in each group. Five regions within per

section were randomly selected, and the number of damaged pyramidal neurons was counted. The morphology of damaged pyramidal neurons displayed nuclear pyknosis.

Nissl Staining

Paraffin sections were deparaffinized, hydrated, and stained with 1% thionine (Sangon Biotech, Shanghai, China) for 30 min. The sections were placed in increasing concentrations of ethyl alcohol (70, 80, 90, and then 100%) for 2 min each, followed by xylene twice (10 min each) at RT. Images were captured under a light microscope (Nikon Corporation, Tokyo, Japan) and brain neuronal damage was analysed by observation of histological changes in the hippocampal CA1 subfield in all 5 rats in each group.

Terminal Deoxynucleotidyl Transferase dUTP Nick End Labeling (TUNEL)

Paraffin sections were deparaffinized, hydrated, and incubated with Proteinase K (10 μg/mL in 10 mM Tris/HCl, pH 7.5) for 30 min at RT. TUNEL assay was performed in the hippocampal CA1 subfield using an In Situ Cell Death Detection Kit (Roche, Basel, Switzerland). The sections were captured under a fluorescence microscope (DMI6000B; Leica Microsystems GmbH) from all 5 rats in each group. Five regions within per section were randomly selected for counting TUNEL-positive cells using ImageJ software (version 5.0; National Institutes of Health). Apoptosis index = (apoptotic cell number/total cells) × 100% [37].

Quantitative Real-Time Polymerase Chain Reaction (qRT-PCR) Assay

Total RNAs were extracted from rat hippocampi tissues using a High Pure Tissue RNA extraction kit (Sigma-Aldrich) and reversed transcribed into cDNA using a PrimeScript™ RT Reagent Kit (TaKaRa, Dalian, China). PCR was performed using TB Green® Fast qPCR Mix (TaKaRa) with the following primers: *Tnf-α* forward, 5′-ATGGGC TCCCTCTCATCAGT-3′, reverse, 5′- GCTTGGTGGTTT GCTACGAC-3′; *Il-6* forward, 5′- AGAGACTTCCAGCCA GTT GC-3′, reverse, 5′-TGCCATTGCACAACTCTTTTC-3′; *Il-1β* forward, 5′-GGGCC TCAAGGGGAAGAATC-3′, reverse, 5′-TTTGGGATCCACACTCTCCAG-3′; *Il-18* forward, 5′- CAGCTCTTCTACCAGCAAACAT-3′, reverse, 5′-CTTCCAACTGAG AGGCTGTGC-3′; β-actin forward, 5′-CCGCGAGTACAACCTTCTTG-3′, reverse, 5′-CGTCAT CCATGGCGAACTGG-3′.

SH-SY5Y Cell Culture

SH-SY5Y cells were purchased from Procell Life Science & Technology Co., Ltd. (Wuhan, China) and cultured in Minimum Essential Medium (MEM)/F12 (Procell Life Science & Technology Co., Ltd.) supplemented with 15% fetal bovine serum (HyClone) and 1% penicillin/streptomycin solution (Gibco). For oxygen–glucose deprivation/reoxygenation (OGD/R) induction, SH-SY5Y cells were cultured in 6-well plates in glucose-free culture medium. After 6 h of incubation in an oxygen-deficient environment (5% CO_2, 1% O_2, and 94% N_2) in an incubator (Version PH-1-A; Puhe Biomedical Technology Co., LTD., Wuxi, China) at 37 °C, the cells were returned to normal culture conditions for another 24 h to reoxygenate.

Co-culture of SH-SY5Y Cells and hUC-MSCs

For co-culture experiments, a 6-well Transwell® chamber (Millipore, Bedford, MA, USA) with 0.4 μm pores was used, as previously described [38]. Briefly, 5×10^5 OGD/R-treated SH-SY5Y cells and/or VCAM-1^- hUC-MSCs / VCAM-1^+ hUC-MSCs (3 independent hUC-MSCs) were seeded in the lower and upper sides of the chamber. The indicated cells were maintained at 37 °C and 5% CO_2.

Cell proliferation-Associated CCK-8 Analysis

The proliferative potential of SH-SY5Y cells was analysed by Cell Counting Kit 8 (Dojindo Molecular Technologies, Kyushu, Japan) assay after 0, 12, 24, and 48 h of co-culturing. Briefly, SH-SY5Y cells were washed twice with 1 × PBS and 10 μL CCK-8 solution was then added for a 4 h of incubation at 37 °C. The absorbance at 450 nm (A450) of each well was recorded using a microplate reader (Bio-Rad Laboratories, Hercules, CA, USA). The survival rate was calculated based on the absorbance values.

Apoptosis Assay

The percentage of apoptotic SH-SY5Y cells was determined using an Annexin V-FITC Apoptosis Detection Kit (Beyotime) according to the manufacturer's instructions after 48 h of co-culture. At least 1×10^5 SH-SY5Y cells were harvested into 195 μL Binding Buffer and stained with 5 μL Annexin V-FITC and 10 μL PI at RT in the dark for 15 min. Apoptotic cells were detected by flow cytometry (BD Biosciences, San Jose, CA, USA) and analysed using FlowJo software (Treestar, San Carlos, CA, USA).

Enzyme-Linked Immunosorbent Assay (ELISA)

Following 48 h of co-culturing, the culture medium of SH-SY5Y cells was collected and the TNF-α, IL-6, IL-1β, and IL-18 levels were analysed using ELISA kits (Nanjing Jiancheng Bioengineering Institute, Nanjing, China) according to the manufacturer's instructions.

Western Blot Assay

Total protein was extracted from cerebral cortex tissues and SH-SY5Y cells using RIPA lysis buffer (Beyotime). The protein extracts were subjected to sodium dodecyl sulfate–polyacrylamide gel electrophoresis (30 μg per lane) and transferred onto polyvinylidene fluoride membranes (Millipore). After blocking with 5% skimmed milk for 1 h at RT, the membranes were incubated with primary anti-TNF-α (1:1000, ab183218, Abcam), anti-IL-6 (1:1000, ab233706, Abcam), anti-IL-1β (1:1000, ab234437, Abcam), anti-IL-18 (1:1000, #67,775, Cell Signaling Technology), anti-NLRP3 (1:1000, ab263899, Abcam), anti-Caspase-1 (1:1000, #24,232, Cell Signaling Technology), anti-ASC (1:2000, 10,500–1-AP, Proteintech), anti-GSDMD-N (1:1000, ab215203, Abcam), and anti-β-actin (1:20,000, 66,009–1-Ig, Proteintech) antibodies overnight at 4 °C. The membranes were incubated with secondary antibodies (1:2000, Abcam) for 1 h at RT, and the blots were developed using BeyoECL Plus (Beyotime).

Cell Transfection

SH-SY5Y cells in 24-well plates (1×10^5 cells/well) were incubated with 6 μg/mL polybrene and infected with lentivirus expressing NLRP3 (FulenGen, Guangzhou, China) at a multiplicity of infection (MOI) of 10. Control cells were infected with virus containing empty vector. After 24 h of incubation at 37 °C, the medium was replaced and the cells were cultured for another 72 h at 37 °C.

Statistical Analysis

All statistical analyses were performed using Prism 6.0 (GraphPad Software). Comparisons between two groups were analysed using an unpaired *t*-test, while comparisons among multiple groups were conducted using one- or two-way ANOVA. A statistically significant difference was considered when the *P*-value was less than 0.05. All data are presented as mean ± SD. In vitro data were obtained from three independent experiments in triplicate. *, $P < 0.05$; **, $P < 0.01$; ***, $P < 0.001$; ns, not significant.

Results

Characteristics of VCAM-1$^+$ hUC-MSCs

For the generation of VCAM-1$^+$ hUC-MSCs, we took advantage of the "3ILs"-based strategy, as we recently reported [12]. The cultured UC-MSCs with a minimal percentage of VCAM-1$^+$ MSCs (< 3%) are referred to as VCAM-1$^-$ UC-MSCs, whereas the counterparts with a higher percentage of VCAM-1$^+$ MSCs (> 85%) are referred to as VCAM-1$^+$ UC-MSCs, as we reported before [12].

To evaluate the transcriptomic signatures of VCAM-1$^+$ hUC-MSCs, we performed RNA-seq and bioinformatics analyses based on the differentially expressed genes (DEGs) between VCAM-1$^+$ UC-MSCs and their VCAM-1$^-$ counterparts. Gene ontology (GO) analysis of the significantly upregulated genes in VCAM-1$^+$ hUC-MSCs revealed that, they are mainly involved in vascularization- and immunoregulation-associated biological processes, such as ECM organization, and neuronal system, cerebrovascular disease, and collagen formation (Fig. 1a). KEGG analysis showed that a series of immunoregulation-associated signaling pathways were enriched based on the DEGs, including interferon (IFN), interleukin (IL), and TCR signaling (Fig. 1b). The upregulated DEGs in VCAM-1$^+$ UC-MSCs are involved in metalloendopeptidase activity, extracellular matrix structural constituents, and positive regulation of nervous development (Fig. 1c). The downregulated DEGs are principally associated with chemokine receptor binding, the type I interferon signaling pathway, the IFN-γ-mediated signaling pathway, and the cellular response to IFN-γ (Fig. 1d). Consistently, as shown by the GSEA diagrams, we observed specific enrichment of vessel-associated subsets (e.g., dilated cardiomyopathy, coronary microvascular disease), together with the mannose type O-lycan biosynthesis-, immunoglobulin complex-, and sulfotransferase activity-associated subsets between the VCAM-1$^+$ and VCAM-1$^-$ groups (Fig. 1e, f). Taken together, the generated VCAM-1$^+$ hUC-MSCs exhibited multifaceted transcriptomic features in immunomodulation, neuronal system, and vessel-associated gene sets compared to those of the parental VCAM-1$^-$ counterparts, which collectively indicates their potential superiority in neuroprotection, including cerebral infarction-associated dysfunction.

VCAM-1$^+$ hUC-MSCs Revealed Improved Effect Against Cerebral Infarction in Rats

Having obtained preliminary verification of the enhanced attributes over the VCAM-1$^-$ subset, we explored the potential efficacy of VCAM-1$^+$ hUC-MSCs for cerebral

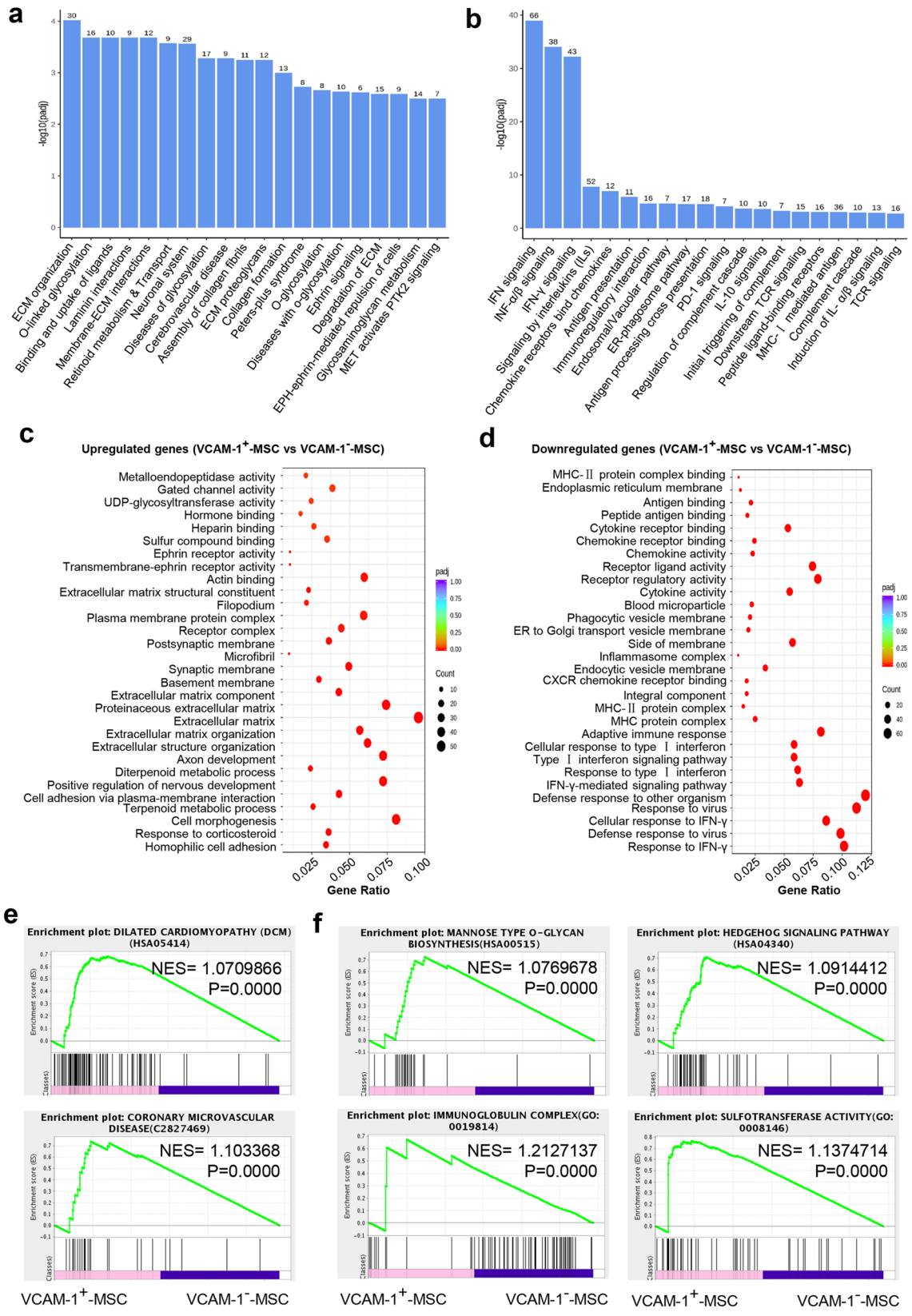
a
-log10(padj)
ECM organization
O-linked glycosylation
Binding and uptake of ligands
Laminin interactions
Membrane-ECM interactions
Retinoid metabolism & Transport
Neuronal system
Diseases of glycosylation
Cerebrovascular disease
Assembly of collagen fibrils
ECM proteoglycans
Collagen formation
Peters-plus syndrome
O-glycosylation
Diseases with o-glycosylation
Ephrin signaling
Degradation of ECM
EPH-ephrin-mediated repulsion of cells
Glycosaminoglycan metabolism
MET activates PTK2 signaling
b
-log10(padj)
IFN signaling
INF-α/β signaling
IFN-γ signaling
Signaling by interleukins (ILs)
Chemokine receptors bind chemokines
Antigen presentation
Immunoregulatory interaction
Endosomal/Vacuolar pathway
ER-phagosome pathway
Antigen processing cross presentation
PD-1 signaling
Regulation of complement cascade
IL-10 signaling
Initial triggering of complement
Downstream TCR signaling
Peptide ligand-binding receptors
MHC- I mediated antigen
Complement cascade
Induction of IL- α/β signaling
TCR signaling
c
Upregulated genes (VCAM-1+-MSC vs VCAM-1--MSC)
Metalloendopeptidase activity
Gated channel activity
UDP-glycosyltransferase activity
Hormone binding
Heparin binding
Sulfur compound binding
Ephrin receptor activity
Transmembrane-ephrin receptor activity
Actin binding
Extracellular matrix structural constituent
Filopodium
Plasma membrane protein complex
Receptor complex
Postsynaptic membrane
Microfibril
Synaptic membrane
Basement membrane
Extracellular matrix component
Proteinaceous extracellular matrix
Extracellular matrix
Extracellular matrix organization
Extracellular structure organization
Axon development
Diterpenoid metabolic process
Positive regulation of nervous development
Cell adhesion via plasma-membrane interaction
Terpenoid metabolic process
Cell morphogenesis
Response to corticosteroid
Homophilic cell adhesion
padj
Count
Gene Ratio
d
Downregulated genes (VCAM-1+-MSC vs VCAM-1--MSC)
MHC- II protein complex binding
Endoplasmic reticulum membrane
Antigen binding
Peptide antigen binding
Cytokine receptor binding
Chemokine receptor binding
Chemokine activity
Receptor ligand activity
Receptor regulatory activity
Cytokine activity
Blood microparticle
Phagocytic vesicle membrane
ER to Golgi transport vesicle membrane
Side of membrane
Inflammasome complex
Endocytic vesicle membrane
CXCR chemokine receptor binding
Integral component
MHC- II protein complex
MHC protein complex
Adaptive immune response
Cellular response to type I interferon
Type I interferon signaling pathway
Response to type I interferon
IFN-γ-mediated signaling pathway
Defense response to other organism
Response to virus
Cellular response to IFN-γ
Defense response to virus
Response to IFN-γ
padj
Count
Gene Ratio
e
Enrichment plot: DILATED CARDIOMYOPATHY (DCM) (HSA05414)
NES= 1.0709866
P=0.0000
Enrichment plot: CORONARY MICROVASCULAR DISEASE(C2827469)
NES= 1.103368
P=0.0000
f
Enrichment plot: MANNOSE TYPE O-GLYCAN BIOSYNTHESIS(HSA00515)
NES= 1.0769678
P=0.0000
Enrichment plot: IMMUNOGLOBULIN COMPLEX(GO: 0019814)
NES= 1.2127137
P=0.0000
Enrichment plot: HEDGEHOG SIGNALING PATHWAY (HSA04340)
NES= 1.0914412
P=0.0000
Enrichment plot: SULFOTRANSFERASE ACTIVITY(GO: 0008146)
NES= 1.1374714
P=0.0000
VCAM-1+-MSC
VCAM-1--MSC
VCAM-1+-MSC
VCAM-1--MSC
VCAM-1+-MSC
VCAM-1--MSC

◂**Fig. 1** Transcriptomic characteristics of VCAM-1$^+$ and VCAM-1$^-$ hUC-MSCs. **a**, **b** The biofunction prediction of upregulated **a** and downregulated **b** DEGs based on the -log10(padj) values of the indicated DEGs in VCAM-1$^+$ and VCAM-1$^-$ hUC-MSCs. The numbers of DEGs in the indicated subsets were labeled above the charts. **c**, **d** The gene ontology (GO) analysis of the upregulated (**c**) and downregulated (**d**) DEGs between the VCAM-1$^+$ and VCAM-1$^-$ hUC-MSCs as described in the "Materials and Methods" section. **e**, **f** GSEA showed the enrichment of the specific gene set enrichment based on the values of the indicated genes expressed in VCAM-1$^+$ and VCAM-1$^-$ hUC-MSCs according to the NES and P values. For instance, the vessel-associated gene sets **(e)** and immunomodulation- and synthesis-associated gene sets **(f)** were specifically enriched by GSEA

infarction administration. Therefore, we took advantage of the Sprague–Dawley rat model of middle cerebral artery occlusion (MCAO) and intravenously infused 4×10^6 VCAM-1$^-$ and VCAM-1$^+$ hUC-MSCs 4 h post-MCAO surgery, respectively (Fig. 2a). Compared to the normal control group (referred to as Sham), the other three groups (MCAO, MCAO + VCAM-1$^-$, and MCAO + VCAM-1$^+$) had higher mNSS scores without significant differences on day 1 of the model (Fig. 2b). Instead, the mNSS scores of MCAO rats with administration of hUC-MSCs (VCAM-1$^-$ and VCAM-1$^+$) were efficiently reduced on day 14 of the model, particularly for the rats treated with VCAM-1$^+$ hUC-MSCs (Fig. 2b).

To further assess the impact of VCAM-1$^+$ hUC-MSC infusion on the amelioration of the learning and memory capacities of MCAO rats, we outperformed a water maze test and found a dynamic decline and distinctions in the escape latency between the MCAO + VCAM-1$^-$ group and the MCAO + VCAM-1$^+$ group (Fig. 2c). Consistently, the decreased time in the target quadrant and the crossing times in the MCAO group were more conspicuously rescued in the MCAO + VCAM-1$^+$ group than in the MCAO + VCAM-1$^-$ group, indicating the amelioration in learning and memory capacities after systemic VCAM-1$^+$ hUC-MSC treatment (Fig. 2d e). Furthermore, by TTC staining, we observed a more effective mitigation of the cerebral infarct volume in MCAO rats with VCAM-1$^+$ hUC-MSCs infusion compared to those with the parental VCAM-1$^-$ hUC-MSCs (Fig. 2f, g). Collectively, the single application of VCAM-1$^+$ hUC-MSCs was sufficient for improving the learning and memory capacities of rats with cerebral infarction.

VCAM-1$^+$ hUC-MSCs Exhibited Improved Neuroprotective Effects on Rats with Cerebral Infarction

For detailed dissection of the therapeutic effects of VCAM-1$^+$ hUC-MSCs on cerebral infarction, we conducted histological assessment of the brain tissues in the indicated groups after euthanasia on day 14 of the model. According to the H&E staining, MCAO rats treated with VCAM-1$^+$ hUC-MSCs exhibited a decrease in brain tissue damage compared to those treated with the corresponding VCAM-1$^-$ parental MSCs, which was further confirmed by Nissl staining of the neurons (Fig. 3a, b). Meanwhile, we observed that more cells in the brain tissues of the MCAO group were positive for TUNEL staining, suggesting increased levels of apoptosis compared to the Sham group (Fig. 3c). Instead, MCAO rats after VCAM-1$^+$ hUC-MSC treatment manifested a more significant decline in apoptotic cells according to the calculation of the percentage of damaged neurons and the apoptosis index when compared with the MCAO + VCAM-1$^-$ group (Fig. 3d, e). Therefore, intravenous injection of VCAM-1$^+$ hUC-MSCs resulted in an improved ameliorative effect than that of the paternal VCAM-1$^-$ counterparts on neurological defects resulting from cerebral infarction in rats.

Reduction of the NLRP3-Mediated Inflammatory Response Upon Cerebral Infarction by VCAM-1$^+$ hUC-MSCs Administration

Extensive literature has demonstrated the pivotal role of immunomodulatory effects in mediating the therapeutic effects of MSCs in a variety of relapsed and refractory diseases [15, 39]. Therefore, we hypothesized that the better outcomes in MCAO rats after VCAM-1$^+$ hUC-MSC treatment could be related to anti-inflammatory effects in connection with the neurological impairment. Hence, we detected the expression of pro-inflammatory factors (TNF-α, IL-6, IL-1β, and IL-18) in the rat brain tissues. We found that the upregulation of pro-inflammatory factors induced by MCAO was inhibited upon hUC-MSCs treatment. In particular, VCAM-1$^+$ hUC-MSCs treatment decreased the expression of pro-inflammatory factors when compared to VCAM-1- hUC-MSCs (Fig. 4a, b). In addition, hUC-MSCs treatment inhibited the expression of NLRP3 and the concomitant pyroptosis-associated proteins. VCAM-1$^+$ hUC-MSCs treatment showed an improved effect on inhibiting the expression of NLRP3, Caspase-1, ASC, and GSDMD-N than the VCAM-1$^-$ hUC-MSCs treatment (Fig. 4c). Taken together, these data indicate the improved immunomodulatory features of VCAM-1$^+$ hUC-MSCs over parental VCAM-1$^-$ hUC-MSCs against pro-inflammatory factors and NLRP3-associated pyroptosis in rat brain tissues.

VCAM-1$^+$ hUC-MSCs Co-Culture Inhibited Cell Death and the NLRP3-Mediated Inflammatory Response in Neuroblastoma Cells

After verifying the in vivo efficacy of VCAM-1$^+$ hUC-MSCs, we explored the beneficial effect on the impaired cellular viability and the underlying NLRP3-associated inflammatory responses. Therefore, we took advantage of the

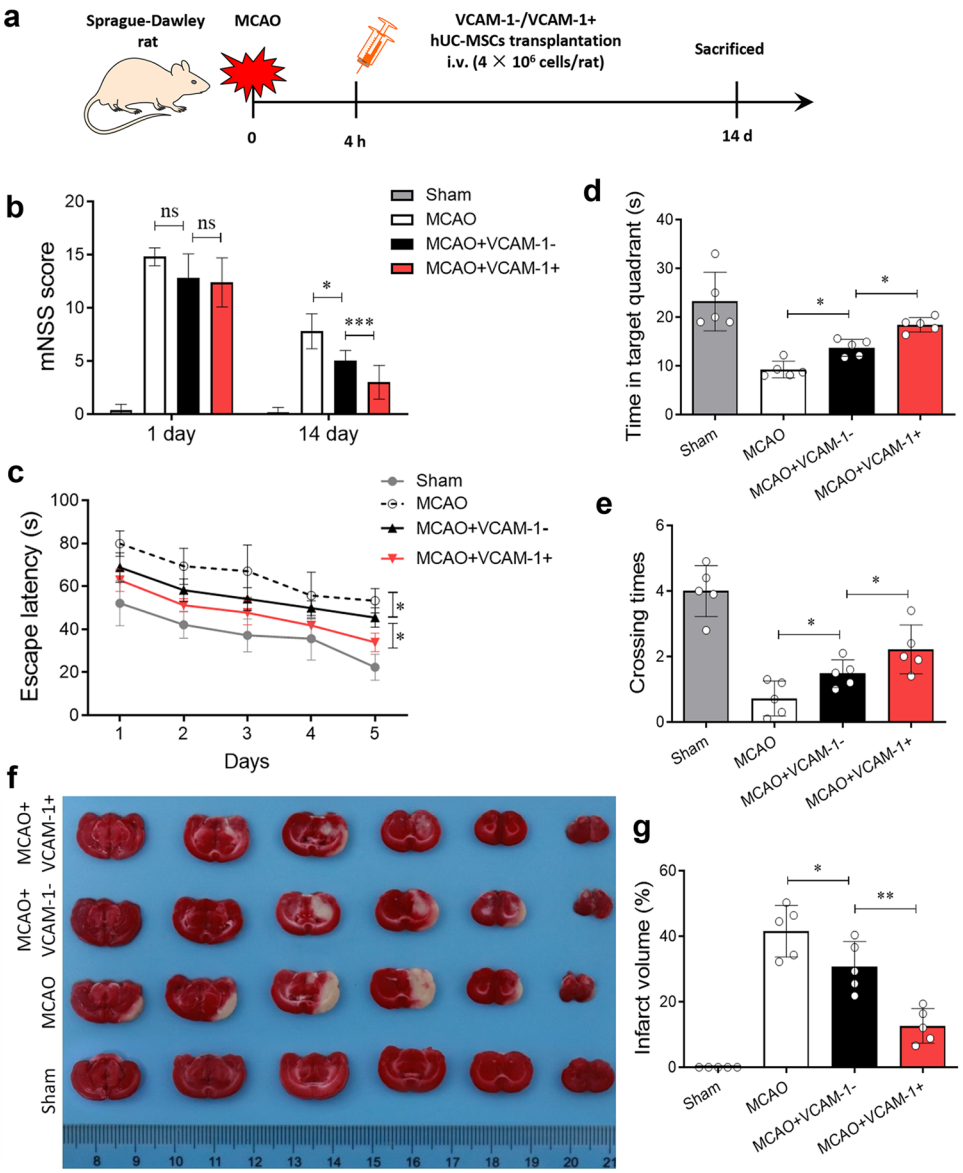

Fig. 2 Improved effects of VCAM-1$^+$ hUC-MSCs against cerebral infarction in rats. **a** Sprague–Dawley rats received intravenous infusion of 4×10^6 VCAM-1$^-$ and VCAM-1$^+$ hUC-MSCs 4 h post-MCAO surgery. **b** Neurological deficits were evaluated using mNSS score on day 1 and 14 post-MCAO surgery. Morris water maze test analysed the **c** average escape latency within 5 days, and the **d** time sated in the target quadrant and **e** crossing time. **f** Representative TTC staining images and **g** the statistical analysis of infarct volumes. Data were shown as mean ± SD (n = 5). *P < 0.05; **P < 0.01; ***P < 0.001; ns, not significant

Transwell assay by co-culturing the OGD/R-treated human SH-SY5Y neural cell line (referred to as OGD/R) with the indicated VCAM-1$^-$ (referred to as OGD/R + VCAM-1$^-$) or VCAM-1$^+$ (referred to as OGD/R + VCAM-1$^+$) hUC-MSCs (Fig. 5a). Compared with the cultured OGD/R-treated SH-SY5Y cells alone, the survival rate of the co-cultured SH-SY5Y cells with VCAM-1$^-$ or VCAM-1$^+$ hUC-MSCs was partially rescued (Fig. 5b). Moreover, as shown by the statistical analyses, SH-SY5Y cells co-cultured with VCAM-1$^+$ hUC-MSCs exhibited a significant decrease in the apoptosis rate (Fig. 5c, d).

To further investigate the anti-inflammatory effects of the indicated MSCs, we measured the concentration of secreted pro-inflammatory factors in the culture supernatant. OGD/R treatment caused a significant increase in the levels of pro-inflammatory factors in the supernatant, whereas the biological phenotype was largely reverted to the level of the control group (referred to as Ctrl) by VCAM-1$^+$ hUC-MSCs rather than by VCAM-1$^-$ hUC-MSCs (Fig. 5e). Moreover, by western-blotting assay, we confirmed the decrease in pro-inflammatory factors and proteins associated with NLRP3-mediated pyroptosis in SH-SY5Y cells in the OGD/R + VCAM-1$^+$ group compared to the OGD/R + VCAM-1$^-$ group (Figs. 5f-g).

NLRP3 Overexpression Prevented the Neuroprotective Effects of VCAM-1$^+$ hUC-MSCs Co-Culture

We overexpressed NLRP3 by lentivirus in SH-SY5Y cells to evaluate the potential effects of NLRP3 on SH-SY5Y cells (Fig. 6a). Western blot analysis revealed a significant

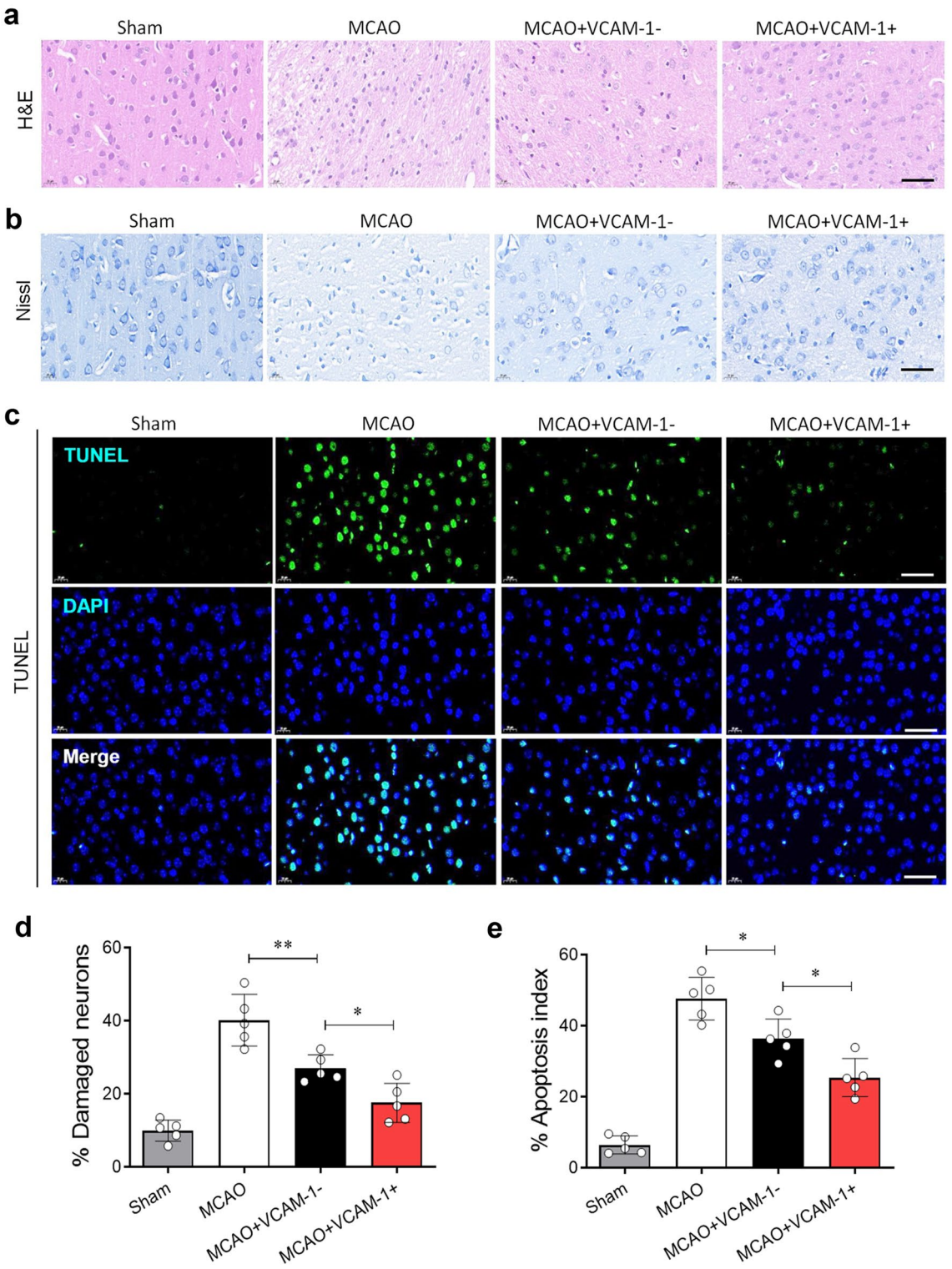

Fig. 3 A better neuroprotective effects of VCAM-1$^+$ hUC-MSCs on rats with cerebral infarction. Representative **a** H&E **b** Nissl, and **c** TUNEL staining images. Scale bar = 50 μm. Statistical analysis of **d** damaged neurons and **e** apoptosis index from H&E and TUNEL staining, respectively. Data were shown as mean ± SD (n = 5). *P < 0.05; **P < 0.01

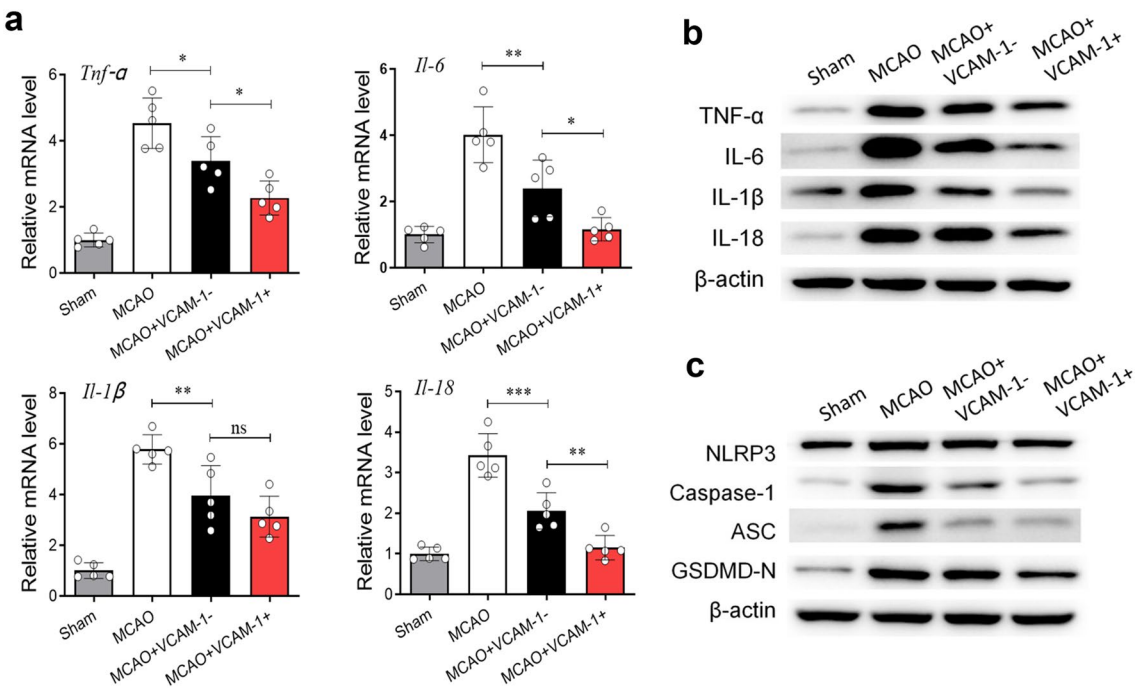

Fig. 4 VCAM-1$^+$ hUC-MSCs inhibited NLRP3-mediated inflammatory response during cerebral infarction in rats. **a** qRT-PCR analysis of pro-inflammatory factors (*Tnf-α*, *Il-6*, *Il-1β*, and *Il-18*) in the rat brain tissues. Western blotting analysis of **b** pro-inflammatory proteins and **c** NLRP3 inflammasome-associated proteins (NLRP3, Caspase-1, ASC, and GSDMD-N) in the rat brain tissues. Data were shown as mean ± SD (n = 5). *P < 0.05; **P < 0.01; ***P < 0.001; ns, not significant

increase in the expression of inflammatory factors in the NLRP3-overexpressing groups compared to that in the corresponding negative control groups (Fig. 6b). Furthermore, as shown by the FCM diagrams, the apoptosis rate of NLRP3-overexpressing SH-SY5Y cells co-cultured with the VCAM-1$^-$ or VCAM-1$^+$ hUC-MSCs was higher than that of the corresponding parental hUC-MSCs (Fig. 6c, d). Overall, these data indicated that the beneficial effects of VCAM-1$^-$ as well as VCAM-1$^+$ hUC-MSC co-culture could be prevented by NLRP3 overexpression in SH-SY5Y cells.

Discussion

Cerebral infarction has been recognized as a common complication in a variety of disorders such as bacteremic infections, sickle cell disease [40], acute anemia [41], nephrotic syndrome [42], and stroke [43], which are the most common consequences of arterial embolism and cause considerable morbidity and mortality. Despite the establishment of the underlying pathophysiological basis and rapid progress in cerebral infarction treatment remedies, further development of therapeutic options for cerebral neuroprotection is still lacking. In this study, we utilized MCAO rats to mimic the symptoms of cerebral infarction, and we verified the improved efficacy of VCAM-1$^+$ hUC-MSC-based cytotherapy for neuroprotection relative to parental VCAM-1$^-$ hUC-MSCs. Furthermore, our findings highlight the beneficial effect of VCAM-1$^+$ hUC-MSCs on cerebral infarction by suppression of NLRP3-induced pyroptosis and the inflammatory response in a cell model of cerebral infarction.

MSCs are heterogeneous multilineage cells, that are suitable "seed cells" for cytotherapy and tissue engineering [44, 45]. For instance, we and other investigators have verified the feasibility of combining biomaterials or scaffolds with MSC- or MSC-derived exosomes/small extracellular vesicles (sEVs) for relapse and recurrent disease management, such as osteoarthritis [21], wound healing [46], repair of the uterine endometrium [47], and Alzheimer's disease [48]. Generally, MSCs are a rich source of therapeutical EVs [49]. MSCs function by orchestrating a series of patterns, including direct or indirect differentiation, paracrine or autocrine, bidirectional immunoregulation, and by serving as constitutive microenvironments [50, 51]. For example, Li et al. reported a beneficial effect of MSC-derived exosomal lncRNA H19 in promoting wound healing in diabetic foot ulcers by regulating PTEN/microRNA-152-3p [52]. Yu et al. verified that exosomes generated from atorvastatin-pretreated MSCs accelerated angiogenesis during diabetic wound repair by modulation of the AKT/eNOS pathway [53]. Here, we demonstrated the therapeutic effect of VCAM-1$^-$ and VCAM-1$^+$ hUC-MSCs on the management

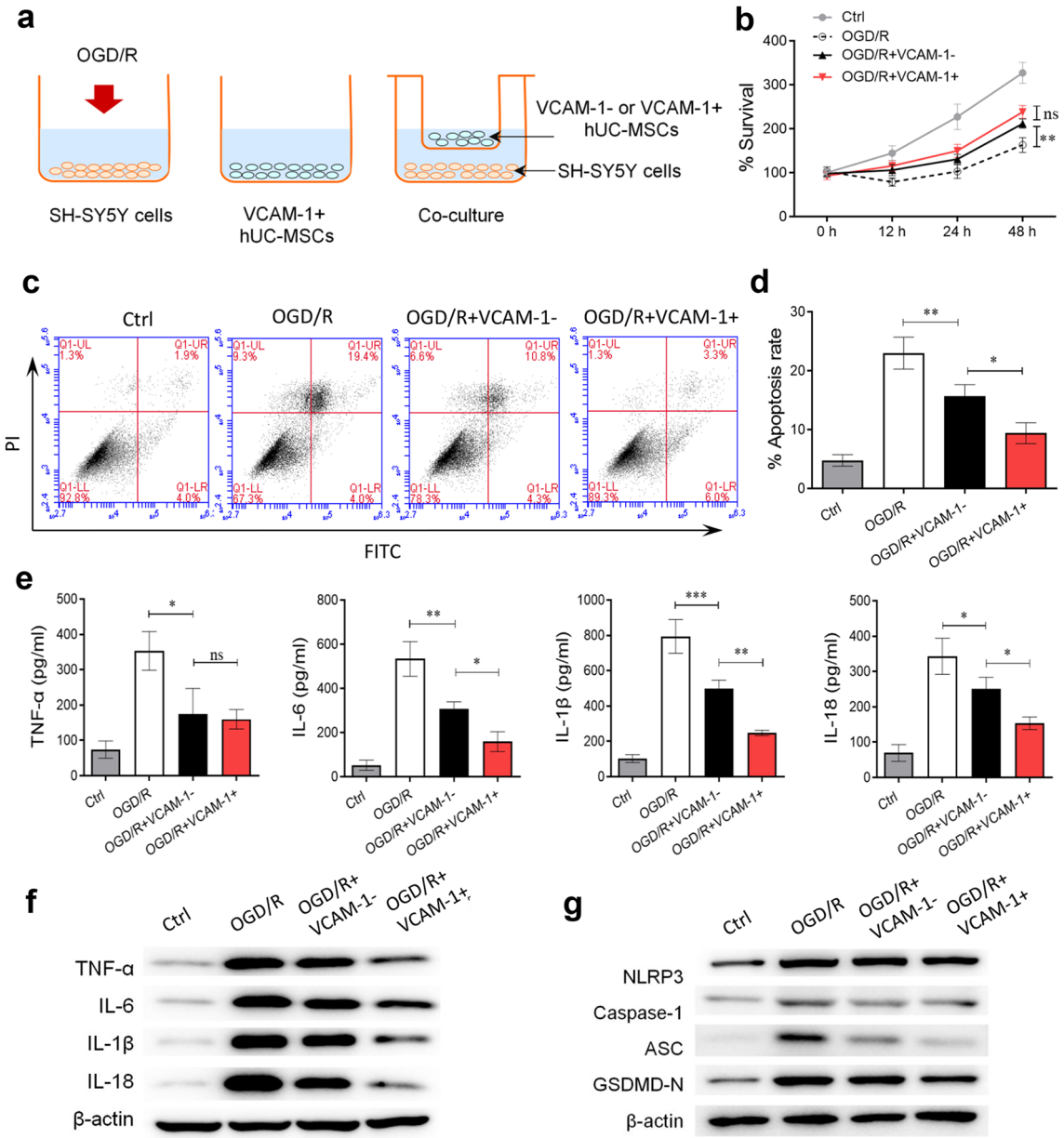

Fig. 5 VCAM-1$^+$ hUC-MSCs co-culture inhibited cell death and the NLRP3-mediated inflammatory response in SH-SY5Y cells. **a** Co-culture of SH-SY5Y cells and VCAM-1$^+$ hUC-MSCs in a Transwell chamber. **b** Survival of SH-SY5Y cells at 0, 12, 24, and 48 h of co-culturing was tested by CCK-8 assays. **c** Representative FCM analysis and **d** statistical analysis of apoptosis rate. **e** Concentrations of cytokines (TNF-α, IL-6, IL-1β, and IL-18) in the culture supernatant of SH-SY5Y cells were analysed by ELISA. Western blotting analysis of **f** pro-inflammatory proteins and **g** NLRP3 inflammasome-associated proteins (NLRP3, Caspase-1, ASC, and GSDMD-N) in SH-SY5Y cells were detected. Data were shown as mean ± SD (n = 3). *P < 0.05; **P < 0.01; ***P < 0.001; ns, not significant

of a rat model of MCAO possibly via suppression of the generation of pro-inflammatory factors and NLRP3-associated pyroptosis.

VCAM-1 is thought to be a canonical protein associated with inflammation, in addition to participating in the transmigration and adhesion of leukocytes to the interstitium as well as concomitant pathophysiological processes such as tumorigenesis, immunological diseases, autoimmune myocarditis, chronic heart failure, and experimental autoimmune myocarditis (EAM) [54, 55]. Recently, Du et al. verified the feasibility of isolating VCAM-1$^+$ hUC-MSCs with highly bioactive properties, including improved immunomodulation and angiogenesis [26, 56]. Furthermore, we have achieved the highly efficient generation of VCAM-1$^+$ hUC-MSCs using a cytokine-programmed strategy and demonstrated its superiority in the treatment of aplastic anemia

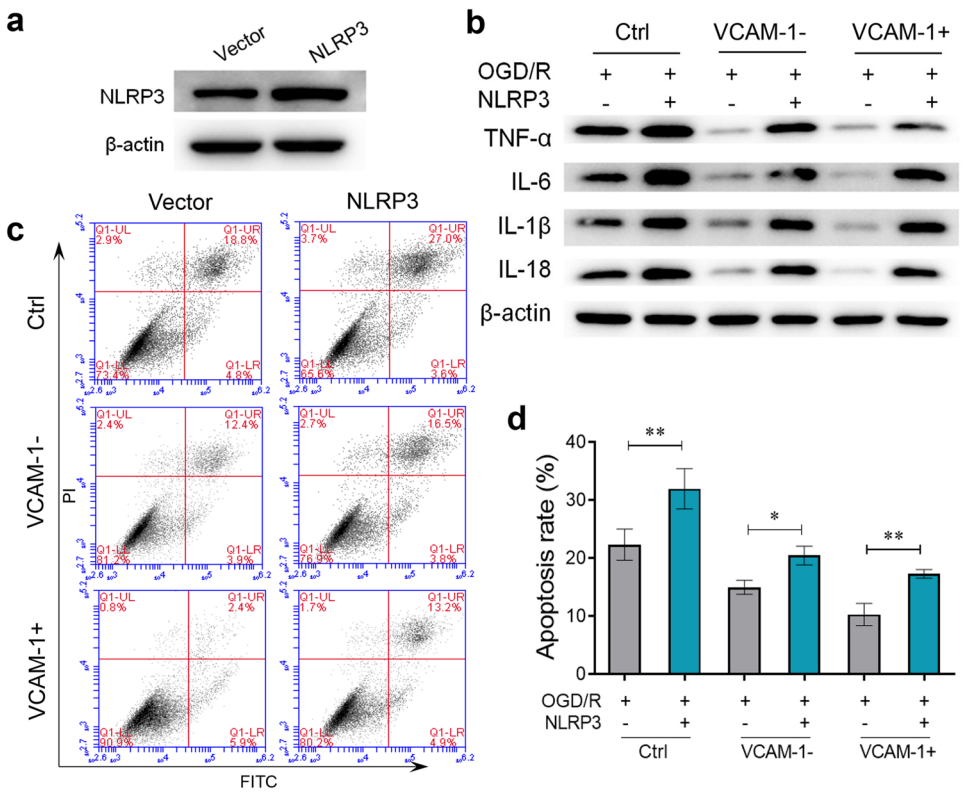

Fig. 6 NLRP3 overexpression prevented the neuroprotective effects of VCAM-1.$^+$ hUC-MSCs co-culture. **a** Western blotting analysis of NLRP3 following SH-SY5Y cells were infected with lentivirus-mediated NLRP3 overexpression. **b** Western blotting analysis of pro-inflammatory proteins (TNF-α, IL-6, IL-1β, and IL-18) in SH-SY5Y cells were detected. **c** Representative FCM analysis and **d** statistical analysis of apoptosis rate. Data were shown as mean ± SD (n = 3). *P < 0.05; **P < 0.01

[12] and acute lung injury [57]. Here, we initially demonstrated the potential of VCAM-1$^+$ hUC-MSCs in neuroprotection against cerebral infarction in rats compared to the VCAM-1$^-$ population. Our data also indicate the underlying mechanism of the NLRP3-induced inflammatory response and pyroptosis, which will collectively benefit the further development of VCAM-1$^+$ hUC-MSC-based therapeutic remedies for cerebral infarction in clinical practices and new drug application (NDA) in the future. Nevertheless, different from the model by Ciobanu et al. with both young and aged Sprague–Dawley rats for mimicking stroke, our study was conducted on young adult male rats, which thus partially limited the reflection of clinical manifestations of stroke in mostly aged and comorbid patients [58]. Collectively, our findings put forward the neuroprotection of VCAM-1$^+$ hUC-MSCs for the management of cerebral infarction and the concomitant mechanism via suppressing NLRP3-induced pyroptosis.

Conclusions

Cerebral infarction causes high morbidity and mortality, resulting in a heavy physical and psychological burden on patients and caregivers. Thus, there is an urgent need to develop novel strategies for efficient remission of cerebral infarction. In this study, we demonstrated the relevance of VCAM-1$^+$ hUC-MSC-based cytotherapy for preclinical neuroprotection against cerebral infarction.

Supplementary Information The online version contains supplementary material available at https://doi.org/10.1007/s11064-023-03968-y.

Acknowledgements The coauthors thank the members in the laboratory research team of the Second Hospital of Shandong University for their professional assistance. We also thank the Key Laboratory of Molecular Diagnostics and Precision Medicine for Surgical Oncology in Gansu Province & NHC Key Laboratory of Diagnosis and Therapy of Gastrointestinal Tumor in Gansu Provincial Hospital, and Key Laboratory of Radiation Technology and Biophysics, Hefei Institute of Physical Science in Chinese Academy of Sciences for their technical support.

Authors' contributions X.Z. and P.W.: designed and performed the experiments, collection and assembly of data, manuscript writing; X.S., Y.C., H.Y., Y.S., X.L., X.L.Z., X.W., H.Y., and J.B.: helped with experiments, collection and assembly of data; X.Z., L.Z., and P.W.: data analysis and interpretation, manuscript writing; L.Z., and P.W.: conception and design, revision, final approval of manuscript. All coauthors have read and approved the final manuscript.

Funding This work was supported by grants from the National Natural Science Foundation of China (81870848, 82260031, 82171410), Rongxiang Regenerative Medicine Foundation of Shandong University (No. 2019SDRX-09), Jinan clinical medical science and technology innovation program (201907056, 202134018), Foundation of the Second Hospital of Shandong University (2022YP93), the project Youth Fund supported by Shandong Provincial Natural Science Foundation (ZR2020QC097), Jiangxi Provincial Natural Science Foundation

(20224BAB206077, 20212BAB216073), Jiangxi Provincial Leading Talent of "Double Thousand Plan" (2022 to L.S.Z.).

Data availability All data generated or analysed during this study, together with the additional file, are included in this published article. Meanwhile, the datasets involved in the current study are available from the corresponding author on reasonable request.

Declarations

Conflict of Interest The coauthors declare there's no competing interests and all the coauthors consent to publish the data.

Ethics Approval and Consent to Participate This study was performed according to the principle of Declaration of Helsinki. Meanwhile, ethical approval of this research was approved by the Ethics Committee of Institutional Animal Care and Use Committee of the Second Hospital of Shandong University to the National Institutes of Health (NIH) guidelines for the Care and use of Laboratory Animals(Ethics approval No. KYLL-2022LW157).

Consent for Publication Not applicable.

References

1. Arboix A, Alio J (2012) Acute cardioembolic cerebral infarction: answers to clinical questions. Curr Cardiol Rev 8(1):54–67
2. who.int.: STEPwise approach to stroke surveillance, 2013. [updated 10 August, 2013; cited 10 August, 2013]. Available at http://www.who.int/chp/steps/stroke/en/. In.; 2013.
3. Guzik A, Bushnell C: Stroke Epidemiology and Risk Factor Management. *Continuum (Minneapolis, Minn)* 2017, 23(1, Cerebrovascular Disease):15–39.
4. Yaggi HK, Concato J, Kernan WN, Lichtman JH, Brass LM, Mohsenin V (2005) Obstructive sleep apnea as a risk factor for stroke and death. N Engl J Med 353(19):2034–2041
5. Hurford R, Sekhar A, Hughes TAT, Muir KW (2020) Diagnosis and management of acute ischaemic stroke 20(4):304–316
6. Wu S, Wu B, Liu M, Chen Z, Wang W, Anderson CS, Sandercock P, Wang Y, Huang Y, Cui L et al (2019) Stroke in China: advances and challenges in epidemiology, prevention, and management. The Lancet Neurology 18(4):394–405
7. Azad TD, Veeravagu A, Steinberg GK (2016) Neurorestoration after stroke. Neurosurg Focus 40(5):E2
8. Zhang L, Wang H, Liu C, Wu Q, Su P, Wu D, Guo J, Zhou W, Xu Y, Shi L et al (2018) MSX2 Initiates and Accelerates Mesenchymal Stem/Stromal Cell Specification of hPSCs by Regulating TWIST1 and PRAME. Stem Cell Reports 11(2):497–513
9. Zhao Q, Zhang L, Wei Y, Yu H, Zou L, Huo J, Yang H, Song B, Wei T, Wu D et al (2019) Systematic comparison of hUC-MSCs at various passages reveals the variations of signatures and therapeutic effect on acute graft-versus-host disease. Stem Cell Res Ther 10(1):354
10. Nombela-Arrieta C, Ritz J, Silberstein LE (2011) The elusive nature and function of mesenchymal stem cells. Nat Rev Mol Cell Biol 12(2):126–131
11. Huo J, Zhang L, Ren X, Li C, Li X, Dong P, Zheng X, Huang J, Shao Y, Ge M et al (2020) Multifaceted characterization of the signatures and efficacy of mesenchymal stem/stromal cells in acquired aplastic anemia. Stem Cell Res Ther 11(1):59
12. Wei Y, Zhang L, Chi Y, Ren X, Gao Y, Song B, Li C, Han Z, Zhang L, Han Z (2020) High-efficient generation of VCAM-1(+) mesenchymal stem cells with multidimensional superiorities in signatures and efficacy on aplastic anaemia mice. Cell Prolif 53(8):e12862
13. Zhang L, Chi Y, Wei Y, Zhang W, Wang F, Zhang L, Zou L, Song B, Zhao X, Han Z (2021) Bone marrow-derived mesenchymal stem/stromal cells in patients with acute myeloid leukemia reveal transcriptome alterations and deficiency in cellular vitality. Stem Cell Res Ther 12(1):365
14. Hou H, Zhang L, Duan L, Liu Y, Han Z, Li Z, Cao X (2020) Spatio-Temporal Metabolokinetics and Efficacy of Human Placenta-Derived Mesenchymal Stem/Stromal Cells on Mice with Refractory Crohn's-like Enterocutaneous Fistula. Stem Cell Rev Rep 16(6):1292–1304
15. Zhao X, Zhao Y, Sun X, Xing Y, Wang X, Yang Q (2020) Immunomodulation of MSCs and MSC-Derived Extracellular Vesicles in Osteoarthritis. Front Bioeng Biotechnol 8:575057
16. Park HS, Chugh RM, El Andaloussi A, Hobeika E, Esfandyari S, Elsharoud A, Ulin M, Garcia N, Bilal M, Al-Hendy A (2021) Human BM-MSC secretome enhances human granulosa cell proliferation and steroidogenesis and restores ovarian function in primary ovarian insufficiency mouse model. Sci Rep 11(1):4525
17. Tan TT, Toh WS, Lai RC, Lim SK (2021) Practical considerations in transforming MSC therapy for neurological diseases from cell to EV. Exp Neurol 349:113953
18. Liu QW, Li JY, Zhang XC, Liu Y, Liu QY, Xiao L, Zhang WJ, Wu HY, Deng KY, Xin HB (2020) Human amniotic mesenchymal stem cells inhibit hepatocellular carcinoma in tumour-bearing mice. J Cell Mol Med 24(18):10525–10541
19. Xu L, Liu Y, Sun Y, Wang B, Xiong Y, Lin W, Wei Q, Wang H, He W, Wang B et al (2017) Tissue source determines the differentiation potentials of mesenchymal stem cells: a comparative study of human mesenchymal stem cells from bone marrow and adipose tissue. Stem Cell Res Ther 8(1):275
20. Wei Y, Hou H, Zhang L, Zhao N, Li C, Huo J, Liu Y, Zhang W, Li Z, Liu D et al (2019) JNKi- and DAC-programmed mesenchymal stem/stromal cells from hESCs facilitate hematopoiesis and alleviate hind limb ischemia. Stem Cell Res Ther 10(1):186
21. Zhang L, Wei Y, Chi Y, Liu D, Yang S, Han Z, Li Z (2021) Two-step generation of mesenchymal stem/stromal cells from human pluripotent stem cells with reinforced efficacy upon osteoarthritis rabbits by HA hydrogel. Cell Biosci 11(1):6
22. El Omar R, Beroud J, Stoltz JF, Menu P, Velot E, Decot V (2014) Umbilical cord mesenchymal stem cells: the new gold standard for mesenchymal stem cell-based therapies? Tissue Eng Part B Rev 20(5):523–544
23. Colicchia M, Jones DA, Beirne AM, Hussain M, Weeraman D, Rathod K, Veerapen J, Lowdell M, Mathur A (2019) Umbilical cord-derived mesenchymal stromal cells in cardiovascular disease: review of preclinical and clinical data. Cytotherapy 21(10):1007–1018
24. Yan J, Liu T, Li Y, Zhang J, Shi B, Zhang F, Hou X, Zhang X, Cui W, Li J et al (2023) Effects of magnetically targeted iron oxide@polydopamine-labeled human umbilical cord mesenchymal stem cells in cerebral infarction in mice. Aging 15(4):1130–1142
25. Wang W, Ji Z, Yuan C, Yang Y (2021) Mechanism of Human Umbilical Cord Mesenchymal Stem Cells Derived-Extracellular Vesicle in Cerebral Ischemia-Reperfusion Injury. Neurochem Res 46(3):455–467
26. Du W, Li X, Chi Y, Ma F, Li Z, Yang S, Song B, Cui J, Ma T, Li J et al (2016) VCAM-1+ placenta chorionic villi-derived mesenchymal stem cells display potent pro-angiogenic activity. Stem Cell Res Ther 7:49
27. He Y, Hara H, Núñez G (2016) Mechanism and Regulation of NLRP3 Inflammasome Activation. Trends Biochem Sci 41(12):1012–1021
28. Yu ZW, Zhang J, Li X, Wang Y, Fu YH, Gao XY (2020) A new research hot spot: The role of NLRP3 inflammasome activation,

a key step in pyroptosis, in diabetes and diabetic complications. Life Sci 240:117138
29. Jiang N, An J, Yang K, Liu J, Guan C, Ma C, Tang X (2021) NLRP3 Inflammasome: A New Target for Prevention and Control of Osteoporosis? Front Endocrinol 12:752546
30. de Carvalho RM, Szabo G (2022) Role of the Inflammasome in Liver Disease. Annu Rev Pathol 17:345–365
31. Wang Y, Liu X, Shi H, Yu Y, Yu Y, Li M, Chen R: NLRP3 inflammasome, an immune-inflammatory target in pathogenesis and treatment of cardiovascular diseases. 2020, 10(1):91–106.
32. Luo Y, Reis C, Chen S (2019) NLRP3 Inflammasome in the Pathophysiology of Hemorrhagic Stroke: A Review. Curr Neuropharmacol 17(7):582–589
33. Alishahi M, Farzaneh M, Ghaedrahmati F, Nejabatdoust A, Sarkaki A, Khoshnam SE: NLRP3 inflammasome in ischemic stroke: As possible therapeutic target. 2019, 14(6):574–591.
34. Yang X, Wu S (2021) N-oleoylethanolamine - phosphatidylcholine complex loaded, DSPE-PEG integrated liposomes for efficient stroke. Drug Delivery 28(1):2525–2533
35. Wang C, Ma Z, Wang Z, Ming S, Ding Y, Zhou S, Qian H (2021) Eriodictyol Attenuates MCAO-Induced Brain Injury and Neurological Deficits via Reversing the Autophagy Dysfunction. Front Syst Neurosci 15:655125
36. Swanson RA, Morton MT, Tsao-Wu G, Savalos RA, Davidson C, Sharp FR (1990) A semiautomated method for measuring brain infarct volume. Journal of cerebral blood flow and metabolism : official journal of the International Society of Cerebral Blood Flow and Metabolism 10(2):290–293
37. Peng L, Yang C, Yin J, Ge M, Wang S, Zhang G, Zhang Q, Xu F, Dai Z, Xie L et al (2019) TGF-β2 Induces Gli1 in a Smad3-Dependent Manner Against Cerebral Ischemia/Reperfusion Injury After Isoflurane Post-conditioning in Rats. Front Neurosci 13:636
38. Li F, Zhang J, Chen A, Liao R, Duan Y, Xu Y, Tao L (2021) Combined transplantation of neural stem cells and bone marrow mesenchymal stem cells promotes neuronal cell survival to alleviate brain damage after cardiac arrest via microRNA-133b incorporated in extracellular vesicles. Aging 13(1):262–278
39. Zhang L, Dong ZF, Zhang JY (2020) Immunomodulatory role of mesenchymal stem cells in Alzheimer's disease. Life Sci 246:117405
40. Musallam KM, Khoury RA, Abboud MR (2011) Cerebral infarction in children with sickle cell disease: a concise overview. Hemoglobin 35(5–6):618–624
41. Tsai CF, Yip PK, Chen CC, Yeh SJ, Chung ST, Jeng JS (2010) Cerebral infarction in acute anemia. J Neurol 257(12):2044–2051
42. Yun YW, Chung S, You SJ, Lee DK, Lee KY, Han SW, Jee HO, Kim HJ (2004) Cerebral infarction as a complication of nephrotic syndrome: a case report with a review of the literature. J Korean Med Sci 19(2):315–319
43. Zhao Y, Zhang X, Chen X, Wei Y: Neuronal injuries in cerebral infarction and ischemic stroke: From mechanisms to treatment (Review). *Int J Mol Med* 2022, 49(2).
44. Wagenbrenner M, Mayer-Wagner S, Rudert M, Holzapfel BM, Weissenberger M: Combinations of Hydrogels and Mesenchymal Stromal Cells (MSCs) for Cartilage Tissue Engineering-A Review of the Literature. *Gels* 2021, 7(4).
45. Brennan MA, Layrolle P, Mooney DJ: Biomaterials functionalized with MSC secreted extracellular vesicles and soluble factors for tissue regeneration. *Adv Funct Mater* 2020, 30(37).
46. Casado-Diaz A, Quesada-Gomez JM, Dorado G (2020) Extracellular Vesicles Derived From Mesenchymal Stem Cells (MSC) in Regenerative Medicine: Applications in Skin Wound Healing. Front Bioeng Biotechnol 8:146
47. Ji W, Hou B, Lin W, Wang L, Zheng W, Li W, Zheng J, Wen X, He P (2020) 3D Bioprinting a human iPSC-derived MSC-loaded scaffold for repair of the uterine endometrium. Acta Biomater 116:268–284
48. Reza-Zaldivar EE, Hernandez-Sapiens MA, Minjarez B, Gutierrez-Mercado YK, Marquez-Aguirre AL, Canales-Aguirre AA (2018) Potential Effects of MSC-Derived Exosomes in Neuroplasticity in Alzheimer's Disease. Front Cell Neurosci 12:317
49. Gregorius J, Wang C, Stambouli O, Hussner T, Qi Y, Tertel T, Borger V, Mohamud Yusuf A, Hagemann N, Yin D et al (2021) Small extracellular vesicles obtained from hypoxic mesenchymal stromal cells have unique characteristics that promote cerebral angiogenesis, brain remodeling and neurological recovery after focal cerebral ischemia in mice. Basic Res Cardiol 116(1):40
50. Carreras-Planella L, Monguio-Tortajada M, Borras FE, Franquesa M (2019) Immunomodulatory Effect of MSC on B Cells Is Independent of Secreted Extracellular Vesicles. Front Immunol 10:1288
51. Ren J, Liu Y, Yao Y, Feng L, Zhao X, Li Z, Yang L (2021) Intranasal delivery of MSC-derived exosomes attenuates allergic asthma via expanding IL-10 producing lung interstitial macrophages in mice. Int Immunopharmacol 91:107288
52. Li B, Luan S, Chen J, Zhou Y, Wang T, Li Z, Fu Y, Zhai A, Bi C (2020) The MSC-Derived Exosomal lncRNA H19 Promotes Wound Healing in Diabetic Foot Ulcers by Upregulating PTEN via MicroRNA-152-3p. Mol Ther Nucleic Acids 19:814–826
53. Yu M, Liu W, Li J, Lu J, Lu H, Jia W, Liu F (2020) Exosomes derived from atorvastatin-pretreated MSC accelerate diabetic wound repair by enhancing angiogenesis via AKT/eNOS pathway. Stem Cell Res Ther 11(1):350
54. Troncoso MF, Ortiz-Quintero J, Garrido-Moreno V, Sanhueza-Olivares F, Guerrero-Moncayo A, Chiong M, Castro PF, Garcia L, Gabrielli L, Corbalan R et al (2021) VCAM-1 as a predictor biomarker in cardiovascular disease. Biochim Biophys Acta Mol Basis Dis 1867(9):166170
55. Grabmaier U, Kania G, Kreiner J, Grabmeier J, Uhl A, Huber BC, Lackermair K, Herbach N, Todica A, Eriksson U et al (2016) Soluble Vascular Cell Adhesion Molecule-1 (VCAM-1) as a Biomarker in the Mouse Model of Experimental Autoimmune Myocarditis (EAM). PLoS ONE 11(8):e0158299
56. Yang ZX, Han ZB, Ji YR, Wang YW, Liang L, Chi Y, Yang SG, Li LN, Luo WF, Li JP et al (2013) CD106 identifies a subpopulation of mesenchymal stem cells with unique immunomodulatory properties. PLoS ONE 8(3):e59354
57. Zhang L, Zhuo Y, Yu H (2023) Spatio-temporal metabolokinetics and therapeutic effect of CD106(+) mesenchymal stem/stromal cells upon mice with acute lung injury. Cell Biol Int 47(4):720–730
58. Ciobanu O, Elena Sandu R, Tudor Balseanu A, Zavaleanu A, Gresita A, Petcu EB, Uzoni A, Popa-Wagner A (2017) Caloric restriction stabilizes body weight and accelerates behavioral recovery in aged rats after focal ischemia. Aging Cell 16(6):1394–1403

Authors and Affiliations

Xiao Zhang[1] · Xiaoyu Sang[1] · Yanting Chen[1] · Hao Yu[2] · Yuan Sun[3] · Xilong Liang[4] · Xiaolei Zheng[1] · Xiao Wang[1] · Hui Yang[1] · Jianzhong Bi[1] · Leisheng Zhang[5,6,7] · Ping Wang[1]

✉ Leisheng Zhang
leisheng_zhang@163.com

✉ Ping Wang
wping0108@163.com

[1] Department of Neurology, The Second Hospital of Shandong University, Jinan 250033, China

[2] School of Medicine, Nankai University, Tianjin 300071, China

[3] The Second Hospital of Shandong University, Jinan 250033, China

[4] Department of Biostatistics, School of Public Health, Yale University, 38 Crown Street, APT 203, New Haven, CT 06510, USA

[5] Department of Neurosurgery, Qianfoshan Hospital, The First Affiliated Hospital of Shandong First Medical University, Jinan 250014, China

[6] Key Laboratory of Molecular Diagnostics and Precision Medicine for Surgical Oncology in Gansu Province and NHC Key Laboratory of Diagnosis and Therapy of Gastrointestinal Tumor, Gansu Provincial Hospital, Lanzhou 730000, China

[7] Key Laboratory of Radiation Technology and Biophysics, Hefei Institute of Physical Science, Chinese Academy of Sciences, Hefei 230031, China